Investigation of the MgO adsorbate and the MgO/Fe interface on a Fe/GaAs(001) substrate by means of XPS and XPD

D. Handschak[1], T. Lühr[1,2], F. Schönbohm[1,2], C. Keutner[1,2], U. Berges[2] and C. Westphal[1,2]

1 Lehrstuhl für Experimentelle Physik 1, Otto-Hahn-Str. 4
2 DELTA, Maria-Goeppert-Mayer-Str. 2
University of Technology, 44221 Dortmund, Germany

ABSTRACT

We report a combined high-resolution photoemission (XPS) and photoelectron diffraction (XPD) investigation of a magnesium oxide adsorbat on an Fe (1×1) surface, which was prepared on a (4×2)-reconstructed GaAs sample. This study revealed a crystalline MgO film and an iron oxide interface. The examination of the diffraction patterns clearly indicates partially shifted magnesium layers in the halite structure, and a crystalline bcc iron film as subtrate.

Keywords: XPS, XPD, thin film adsorbtion

1 Introduction

Magnesiumoxide is an appliciable insulator in magnetic tunnel junctions (MTJ). The principles of these MTJs are based on the tunnel magneto-resistance, which was discovered by Julière in 1975 [1]. A TMR component is structured of two ferromagnets, preferably iron, which are separated by an insulating layer [2]. The resistivity between the ferromagnetic contacts is strongly depending on the mutual direction of magnetic orientation of the two ferromagnetic layers [3]. This observation is attributed to spin-depending scattering at the ferromagnet/insulator interface [4]. TMR-components are also of interest in the field of research of magnetoresistive random access memories (MRAM) [5]. This non-volatile data storage technique may offer a way of keeping data without permanent energy consumption for the storage mechanism. The structure, especially the interface structure, has a strong influence on the efficiency of the effects [6].

In this paper we report on the structural properties of an MgO layer prepared on an iron film. The iron was evaporated on a (4×2)-reconstructed GaAs sample providing a crystalline Fe (1×1)-surface. In order to investigate the structure of an adsorbate layer x-ray photoelectron diffraction (XPD) was applied. XPD combines core-level photoemission spectroscopy with intensity variations as a function of polar- and azimuth-angle. The out going photoelectron wave of the emitting atom is scattered at the neighboring atoms and resulted in intensity variations of the spectra. Additional high-resolution XPS-spectra allow a detailed analysis for each element and its chemical environment. The spectral components contained in the photoemission signals provide information of the local bonding, e.g. whether the emitter is located as a part of a dimer at the surface or located within a bonding beneath the surface. We compare experimental and simulated XPD patterns for various models. As a result, the crystalline properties of the MgO adsorbate layer grown on Fe/GaAs were confirmed by a comprehensive XPS and XPD analysis. Furthermore, the Fe/MgO-interface is formed by iron oxide adjacent to a partially shifted magnesium film.

2 Experimental Setup

All measurements and the preparation were implemented in an ultra-high vacuum chamber (UHV) with a base pressure of approximately $5 \cdot 10^{-11}$ mbar at beamline 11 at the synchrotron storage ring DELTA in Dortmund, Germany. The chamber contains a hemispherical electron analyzer, an electron beam evaporator, a sputter gun, and a LEED (*low energy electron diffraction*) system. The sample can be moved by a manipulator in all three spatial directions as well as in azimuth and polar angle rotations. Within the XPD measurements polar and azimuth angle were changed evenly, with a polar and azimuth angle range of $60° \geq \theta \geq 0°$ and $0° \leq \phi \leq 360°$, respectively. The step-width of $\Delta\theta = 2°$ and $\Delta\phi = 1.8°$ was kept constant during the measurement. This results in approximately 6000 individual spectra recorded for the hemisphere above the sample. Due to elastic scattering and diffraction effects the intensity of the photoemission signal varies as a function of emission direction [7]. The anisotropy function is defined as $\chi(\theta,\phi) = [I(\theta,\phi) - I_0(\theta)]/I_0(\theta)$ where $I(\theta,\phi)$ and $I_0(\theta)$ denote the intensity at the emission direction (θ,ϕ) and the average intensity at emission direction (θ), respectively [8] [9]. The analysis of the experimental diffraction patterns was implemented by comparing these with simulated patterns obtained for various atom structures. The simulations were performed using the MSPHD program (*full multiple scattering code for low energy photoelectron diffration*), which is an excellent tool for structure investigations [10], [11]. The quantitative comparision between experimental and simulated patterns had been carried out by applying an R-factor

defined as:

$$R = \frac{\sum_i (\chi_{exp_i} - \chi_{sim_i})^2}{\sum_i (\chi^2_{exp_i} - \chi^2_{sim_i})} \,. \qquad (1)$$

In this definition [12] an R-factor of 2 corresponds to an anti-correlated intensity distribution, whereas a perfect agreement is indicated by an R-factor of zero. The simulation had to be performed for a large number of possible atom positions, thus the numerical effort is rather high. In order to reduce the number of calculations a genetic algorithm was applied, using affine transformations for the structure model variations. Genetic algorithms are very suitable tools in structure search in order to minimize the R-factor because they avoid local minima and have been widely used with great success [13]. The data analysis begins with an identification of the various components within a XPS spectrum, which are related to atoms in sub-surface and surface regions. Therefore, two high resolution spectra were compared. The spectra were recorded at polar angles of $\theta = 0°$ and $\theta = 60°$ providing a more bulk and a more surface sensitive photoemission geometry, respectively. These spectra were fitted by using the Gaussian function

$$G(E) = \sum_i \left[A_i \cdot \exp\left(\frac{1}{2} \left[\frac{E - E_i}{\sigma_i} \right]^2 \right) + h_{LS} \cdot A_i \cdot \exp\left(\frac{1}{2} \left[\frac{E - (E_i - f_{LS})}{\sigma_i} \right]^2 \right) \right] , \qquad (2)$$

where A denotes the complex amplitude, σ_i the full width half maximum (FHWM). The parameters h_{LS} and f_{LS} include the heights ratio and the energy shift caused by the spin-orbit-coupling (SOC). In all spectra the intensity of inelastically scattered electrons was removed by a Shirley-background [14]. In order to prepare a crystalline magnesium oxide layer, a suitable substrate is indispensable. Since the iron (1×1)-film grows crystalline on a (4×2)-reconstructed GaAs (001) surface, we used this surface as a substrate template [15]. The GaAs sample was cut from a single-crystalline Te-doped GaAs(001) wafer with an orientation better than 0.05°. After a cleaning procedure in acetone the GaAs samples were transferred to the UHV-chamber. The usual in-situ preparation of the (4×2)-reconstruction was performed by argon sputtering- and annealing-cycles [15]. The iron layer was prepared by electron beam evaporation. During iron deposition the GaAs sample was evenly rotated around its surface normal in order to support a homogeneous film growth. The subsequently recorded LEED pattern showed a well-ordered (1×1) iron surface. The capping MgO adsorbat layer was prepared by MgO evapoartion. Again, the substrate was rotated around its surface normal during evaporation. An estimate of the layer thickness is calculated as described in Ref. [15]. The mean thicknesses are 3 monolayer and 1.5 monolayer for the Fe-film and MgO-film, respectively.

	E_{kin} [eV]	FWHM [eV]	SOC [eV]
F3	123.03	0.57	0.80
F4	120.85	0.79	0.80
M1	125.86	0.50	0.28
M2	124.68	0.35	0.28

Table 1: Parameters of the least squares fits of the core level spectra of Fe 3p and Mg 2p signals. A Gaussian peak shape was assumed for both signals.

3 Results

The Mg 2p and Fe 3p core level spectra are separated by a few eV, as displayed in Fig. 1. Therefore, both peaks were analyzed separately. The parameters of the best least squares fit are summarized in Table 1. For each peak, two components were obtained within

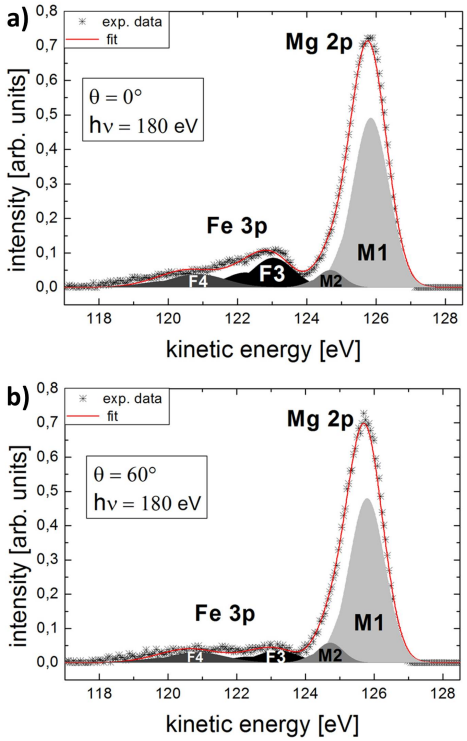

Figure 1: Mg 2p and Fe 3p core level spectra of the prepared MgO adsorbat layer at a polar angle of $\theta = 0°$ (a) and $\theta = 60°$ (b).

the fitting procedure. The magnesium signal contains a strong magnesium component M1 and a small additional component M2, while the iron signal is a superposition of the components F3 and F4, as displayed in Fig. 1. Component M1 corresponds to the ionized magnesium state Mg^{2+}, while component M2 refers to the magne-

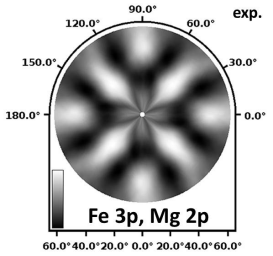

Figure 2: Experimental XPD pattern of Mg 2p and Fe 3p signal, recorded with a photon energy of $h\nu = 180\,\text{eV}$.

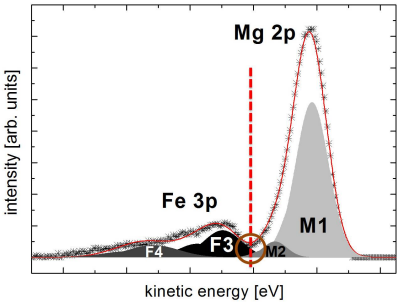

Figure 3: Illustration of the truncation-step applied to the experimental data of the Mg 2p signal. The dashed vertical line (red) denotes the trunctation position within the spectra, while the brown circle indicates the region of strong overlapping of the iron F3 and magnesium M2 components. As a consequence, the Mg 2p diffraction pattern is influenced by the iron signal.

sium bulk signal. In general, the Fe 3p signal decreases with respect to the Mg 2p signal with increasing polar angles. This clearly shows that MgO is the topmost film at the surface. The iron component F3 corresponds to the iron bulk signal since it is strongly decreasing for increasing polar angles. Further, component F4 is shifted by about $\Delta E_{kin} = 2.18$ eV to lower kinetic energies with respect to the iron bulk signal, and it shows a rather weak dependence of the peak intensity as a function of polar angle. This experimental finding is a clear evidence of a possible oxidation of the iron film at the interface resulting from the MgO deposition.

The XPD pattern of the Mg 2p overlapping with the Fe 3p signal is pictured in Fig. 2 and shows a fourfold rotational symmetry. For analyzing the MgO adsorbate layers, the experimental data were reduced to the Mg 2p signal only, as elucidated in Fig. 3. The resulting diffraction pattern of the Mg 2p signal is shown in Fig. 4(a). In the following simulation, MgO is assumed representing a halite structure first with a lattice constant of 4.213 Å. Comparing experimental and simulated diffraction pattern yielded poor agreement only, with an R-factor of $R = 1.14$. However, as a first important result, we found that the strongest intensity lobes

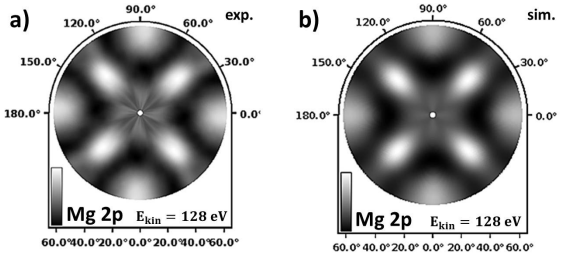

Figure 4: Experimental XPD pattern of the truncated Mg 2p core level signal (a) and its best simulated diffraction pattern (b), based on the structure model as described in the text.

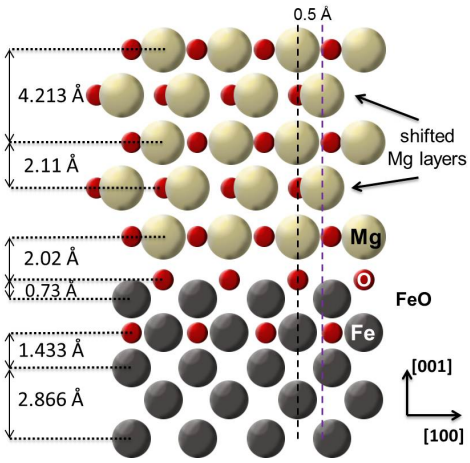

Figure 5: Structure model of the MgO/Fe system of the best simulated patterns obtained for Mg 2p and Fe 3p.

in the pattern were rotated by 45° with respect to the experimental pattern. Although we truncated the spectra, it is not possible to completly remove the iron substrate's influence, because the Gaussian representations of components F3 and M2 still overlap significantly. If the intensity of component F3 will be reduced by a cutoff, then there will also be an intensity reduction in component M2 corresponding to the Mg bulk signal, as illustrated in Fig. 3. Therefore, the structure model had to be modified. In this modified structure, MgO was assumed with the topmost MgO-film being rotated by 45° against an Fe bcc elementary cell with a lattice constant of 2.866 Å. The subsequent simulation for this structure resulted in an R-factor well below 1, indicating this structure as a perfect start for further simulations. Iron oxide is present at the interface which is indicated in the XPS spectra of Fig1. Within the XPD simulations iron oxide was included by various numbers of FeO layers in the structure models. An oxidized iron layer resulting from an MgO adsorbate was prosposed by Meyerheim *et al.* [16] and Yu *et al.* [17]. These authors assume a homogeneous MgO-film at the surface, with an even oxygen content throughout the film. However, in this

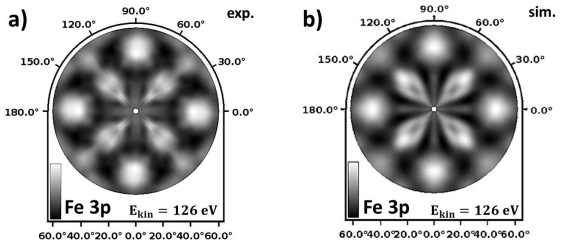

Figure 6: Experimental XPD pattern of the trunctated Fe 3p signal corresponding to the iron layer below MgO (a) and best simulated pattern of the MgO/FeO/Fe structure model (b).

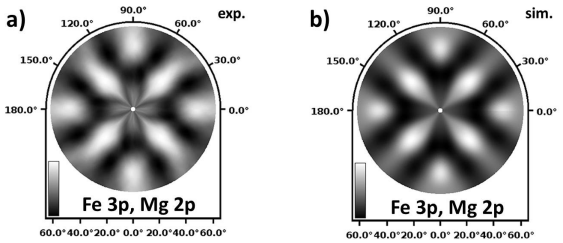

Figure 7: Experimental XPD pattern of the Mg 2p and Fe 3p photoelectron intensity (a) and a superposition of the two best simulated pattern obtained for Mg 2p and Fe 3p (b).

work we found that a film containing more than two iron oxide layers will deteriorate the agreement of experimental and simulated diffraction pattern. In the following structure search the atoms' positions were modified within the genetic algorithm. The best agreement was achieved for a structure model where every second Mg layer was consistently shifted with respect to the others, as shown in Fig. 5. As a consequence, an R-factor of $R = 0.04$ was obtained for this structure indicating a perfect agreement between experimental and simulated pattern. The resulting simulated XPD pattern is shown in Fig 4(b). Encouraged by the results of this model we trunctated the spectra as shown in Fig. 3 and performed a simulation for these data according the model shown in Fig. 5. In this model the iron layers are located under the MgO adsorbate film. Fig. 6(b) displays the obtained results within the simulation. Again, excellent agreement was found and indicated by an R-factor of $R = 0.08$. Additionally, structures with an iron oxide content above and below the equivalent of two iron oxide layers was tried. Summarizing, all these structures led to a very poor agreement between experimental and simulated patterns. Finally, for mixed structures it is possible to superpose the results obtained for two separately calculated diffraction patterns. This procedure was applied to the patterns obtained for Mg 2p and Fe 3p, since a minimal intermixture might be possible. The superposition yielded in a very low R-factor of $R = 0.05$, indicating the perfect agreement with the experimental XPD pattern, as shown in Fig. 7.

4 Conclusion

An MgO-film prepared on a Fe (1×1)-surface on a GaAs (4×2)-reconstructed surface was investigated. The high resolution XPS core level spectra of Mg 2p and Fe 3p prove a successful preparation showing a layered growth. Further, the strong Mg^{2+} state shows that Fe is present in its pristine as well as in an oxidized state. Both, the full MgO capping layer and the MgO/Fe interface grow crystalline on the GaAs template. The different diffraction patterns of the Mg 2p and Fe 3p signal reflect the individual local environment, thus their patterns were analyzed separately first, yielding to a structure model. The analysis of the patterns of the Mg 2p and Fe 3p signals clearly shows an interface structure consisting of two iron oxides layers located on an iron bcc elementary cell. The MgO layer represents a halite structure with the topmost layer rotated by 45° against the Fe layer below, with every second Mg layer being laterally shifted.

We gratefully acknowledge fruitful discussions with H. Krull and thank the DELTA staff for continuous support during beamtimes. This work was supported by the Land Nordrhein-Westfalen, the NRW Forschungsschule and the Bundesministerium für Bildung und Forschung under contract No. 05K10PE2.

REFERENCES

[1] M. Jullière, Phys. Lett. A **54**, 225-226, 1975.
[2] M.S. Xue *et al.*, Vacuum, **85**, 4, 2010
[3] S. Parkin *et.al.*, Nature Materials, **3**, 2004
[4] W.H. Butler *et al.*, Phys. Rev. B, **63**, 054416, 2001
[5] S. Yang *et al.*, Phys. Rev. B, **84**, 184410, 2011
[6] G.X. Du *et al.*, Phys. Rev. B, **81**, 064438, 2010
[7] A. Liebsch, Phys. Rev. Lett., **32**, 1203–1206, 1974
[8] K.-M. Schindler *et al.*, Phys. Rev. B, **46**, 1, 1992
[9] L. Wang *et al.*, Phys. Rev. B, **44**, 3, 1991
[10] R. Gunnella *et al.*, Computer Physics Communications, **132**, 251 - 266, 2000
[11] C.R. Natoli *et al.*, Phys. Rev. B, **42**, 1944–1968, 1990
[12] D.P. Woodruff *et al.*, Rep. Prog. Phys., **57**, 1029, 1994
[13] M.L. Viana *et al.*, J. Phys. Condens. Matter, **19**, 446002, 2007
[14] D.A. Shirley, Phys. Rev. B, **5**, 4709–4714 , 1972
[15] D. Handschak *et al.*, Phys. Rev. B, **submitted**, 2013
[16] H.L. Meyerheim *et al.*, Phys. Rev. Lett., **87**, 076102, 2001
[17] B.D. Yu *et al.*, Phys. Rev. B, **73**, 125408, 2006